ELSEVIER

Chemical Engineering Journal 66 (1997) 171–179

Chemical Engineering Journal

Fly-ash/calcium hydroxide mixtures for SO_2 removal: structural properties and maximum yield

A. Garea, I. Fernández, J.R. Viguri, M.I. Ortiz, J. Fernández, M.J. Renedo, J.A. Irabien *

Departamento de Química, ETSII y T., Universidad de Cantabria, Avda. Los Castros, s/n, 39005 Santander, Spain

Received 12 February 1996; accepted 17 October 1996

Abstract

The structural properties and sulfation capacity of mixed solids obtained from pressurized hydration of commercial calcium hydroxide and coal combustion fly-ashes have been analyzed. Hydration experiments were planned according to a 2^5 fractional factorial design, studying the influence of temperature, time, pressure, fly-ash/$Ca(OH)_2$ weight ratio and water/solid weight ratio, on the BET specific surface area (S) and pore volume (V_p) of the final solids, as well as on the dissolved calcium concentration [Ca] in the slurries.

Whereas a strong dependence of the ratio fly-ash/$Ca(OH)_2$ on (S) and [Ca] functions was observed, with values of these parameters in the ranges 2.5–64.3 $m^2\ g^{-1}$ and 6.0–748.0 mg l^{-1}, respectively, no dependence was found of the studied variables on the pore volume (determined by Hg intrusion porosimetry), obtaining an average value of 1.077 $cm^3\ g^{-1}$.

Sulfation runs using the hydrated solids were conducted in a packed bed reactor with a pure humidified SO_2 gas phase, leading to a constant sulfation yield of 0.56 ± 0.07 mol SO_2 per mol Ca; this yield was independent of the solids specific surface area, and related only to the sorbents calcium content. © 1997 Elsevier Science S.A.

Keywords: Desulfurization; $Ca(OH)_2$/fly-ash sorbents; Structural properties; Sorbent utilization

1. Introduction

Control of sulfur dioxide emissions in large coal-fired plants is performed by three main categories of post combustion techniques, dry sorbent injection, semi-dry systems and wet systems. Direct injection of dry sorbents into the flue gas duct offers an attractive alternative for controlling sulfur dioxide emissions at low temperature, with a technology relatively simple compared to semi-dry or wet methods and with a potential for retrofit applications [1–3].

In-duct injection systems work with a dry powdered sorbent, typically calcium hydroxide, introduced into the humidified flue gas duct downstream of the air preheater and ahead of the particulate collector. Due to the short residence time of the solids in the injection process (1–3 s), a reactive sorbent must be used in order to achieve acceptable levels of SO_2 removal.

A great deal of effort has been devoted to improve sorbent conversion by substituting the conventional hydrated lime by other sorbents. Investigated alternatives included sodium based sorbents such as sodium bicarbonate and sodium sesquicarbonate as well as naturally occurring sodium bicarbonate minerals, Trona and Nahcolita [4,5]. It has also been mentioned that the addition of inorganic deliquescent sodium based salts as potential performance additives to conventional calcium hydrate, can increase the desulfurization rate and sorbent utilization [6–8].

Reactivation and reuse of different types of solids have been evaluated, i.e., lime and recycled spent sorbent [9], boiler limestone or $Ca(OH)_2$ injection solids [10], hydrated lime with silica fume and $Al(OH)_3$ [11] and γ-alumina/calcium sorbents containing metal oxides [12].

Sorbents obtained by mixing lime or $Ca(OH)_2$ with different sources of silica, such as diatomaceous earth, montmorillonitic/bentonitic clays and fly-ash have led to significantly higher conversion of calcium compared to the conversion obtained using hydrated lime [13,14].

The use of fly-ash sorbents in dry FGD systems presents advantages both economically and environmentally, because fly-ash is the most voluminous by-product from all coal-fired power plants [15,16]. The pozzolanic reaction of silica in the fly-ash with $Ca(OH)_2$ in the slurry to form highly hydrated calcium silicates and calcium aluminates has been thought to be responsible for the improvement in solid utilization [17–23].

* Corresponding author. Fax: +34 42 201590; e-mail: irabienj@ccaix3.unican.cs

PII S1385-8947(96)03178-6

It has been reported that an important development of specific surface area takes places in the reactivation of fly-ash at atmospheric pressure, as well as in the treatment of fly-ash by milling and exposing it to a water steam [24,25]. A similar behavior has been observed by slurrying hydrated lime and fly-ash with water at atmospheric pressure and under high pressures [17–21,26–29].

Conversely, the influence of the structural properties of the solid sorbent on the sulfation ability, mainly the specific surface area, has been widely mentioned in the literature [30–32]. A clear influence of the specific surface area on the reaction rate has been reported when using calcium hydroxide as solid sorbent [33–36]. However, the behavior of $Ca(OH)_2$/fly-ash hydrated products has led to divergent conclusions, as a result of the complexity of fly-ash composition and the experimental conditions employed in the hydration step [10,13,18,22,26,27,29,37].

Diffenbach et al. [27], working with $Ca(OH)_2$/fly-ash hydrates obtained under pressurized hydration conditions, pointed out that although the sorbent reactivity increases slightly with specific surface area, similar values of SO_2 uptake were obtained for different ranges of the structural variable.

Peterson and Rochelle's studies [26] focused on the influence of the dissolved calcium concentration in the slurry, concluding that the reactivity increases with the surface area of the product solids, but that high surface area solids are less reactive when they are formed in slurries containing low concentrations of dissolved calcium, suggesting an optimum ratio of calcium to silica. This fact was mentioned elsewhere [18,38], pointing out that calcium silicates can be prepared from fly-ash and other sources of silica with different surface area and reactivity.

Further investigations referring to the use of advanced sorbents corroborated the difficulty in establishing the relationship between specific surface area and sulfation capacity. Jozewicz et al. evaluated reactivated sorbents formed by post furnace injection solids and fly-ash mixtures [10], concluding that the beneficial effect of increased surface area on the removal of SO_2 is dependent on the rate-limiting step (diffusion of SO_2 through the "ash" layer, or chemical reaction). These authors remarked on the importance of highly hydrated species contained in the sorbent surface to the enhanced reactivity of the reactivated solids, and suggested that the release of hydration water upon contact with hot gas provides moisture and new pores, creating a new surface area. This finding was confirmed by working with pressurized hydrated sorbents [14], and was related to the morphological characteristics of the products, differentiating gel-like amorphous surface structures from needle-shaped crystals that contain much less water of hydration than is needed for the sorbent to be reactive with SO_2.

Singer et al. [37] analyzed the suitability of various coal fly-ashes to form the namely ADVAnced siliCATE sorbents from hydration of calcium hydroxide and fly-ashes. Concerning the sulfur dioxide capture, they indicated that the correlation with respect to surface area cannot be used with confidence for all tested sorbents.

Similar conclusions were reported by Hall et al. [19] from bench and pilot-plant results. They pointed out the scattering of the relationship "sorbent reactivity-to-sorbent surface area" for sorbents hydrated under different conditions, evaluating also the effect of the fly-ash source and its previous grinding.

Considering the state of knowledge, this work presents the structural characterization and the sulfation yield of mixed solids prepared by pressurized hydration of commercial $Ca(OH)_2$ and coal combustion fly-ashes. A systematic procedure based on a factorial design of experiments has been applied to the evaluation of hydration variables. Sulfation yield, referred to as "mol SO_2 per mol Ca", has been determined and compared to the results previously reported when using $Ca(OH)_2$ sorbent [33,34,39]. The influence of the solids specific surface area on their sulfation ability has also been evaluated.

2. Experimental

Sorbents were prepared using commercial $Ca(OH)_2$ supplied by Calcinor S.A. and ASTM Class F coal fly-ashes collected in an electrostatic precipitator of Pasajes (Guipuzcoa-Spain), a bituminous coal-fired power plant. The chemical composition and physical properties of these materials, determined in a Leko Instrument, are shown in Table 1.

Sample preparation consisted of the batch pressure hydration of fly-ash/$Ca(OH)_2$/H_2O mixtures in a Parr 4562 stirred stainless steel reactor of 325 cm^3, provided with a Parr 4841 controller. The amount of solid was kept constant at 15 g, selecting the hydration variables: fly-ash/$Ca(OH)_2$ (FA/CH) weight ratio, water/solid (W/S) weight ratio, pressure (p), temperature (T) and time (t). Table 2 summarizes the experimental values of the considered variables.

Table 1
Physicochemical characterization of $Ca(OH)_2$ and fly-ash

Physical properties	Calcium hydroxide	Fly-ash
BET specific surface area ($m^2\ g^{-1}$)	16.2	2.9
Pore volume ($cm^3\ g^{-1}$)	1.206	0.686
Porosity	0.722	0.564
Particle diameter (mean volume) (μm)	4.76	23.44
Skeletal density ($g\ cm^{-3}$)	1.830	1.889
Chemical composition (%)	**Calcium hydroxide**	**Fly-ash**
$SiO_2 + Al_2O_3$ + insolubles	0.70	87.90
Fe_2O_3	0.11	2.67
MgO	0.40	0.24
CaO	2.00	0.84
$Ca(OH)_2$	93.10	–
CO_2	3.90	–
MnO_2	0.01	–
S	0.01	0.16
C + volatiles	–	8.17

Table 2
Experimental design: hydration parameters and results of runs S1 to S17-V

Solid code	Variables					Responses		
	T (°C)	t (h)	FA/CH ($g\,g^{-1}$)	p (MPa)	W/S ($g\,g^{-1}$)	S ($m^2\,g^{-1}$)	V_p ($cm^3\,g^{-1}$)	[Ca] ($mg\,l^{-1}$)
S1	170	1	3/1	1.26	20/1	16.4	1.11	504.0
S2	170	4	3/1	0.84	20/1	41.9	1.13	10.3
S3	110	4	3/1	1.26	20/1	18.4	0.97	297.5
S4	170	4	3/1	1.26	10/1	64.3	1.14	6.0
S5	170	4	1/3	1.26	20/1	2.5	1.08	656.0
S6	110	4	1/3	1.26	10/1	24.8	1.16	587.4
S7	170	4	1/3	0.84	10/1	3.1	1.16	576.1
S8	110	4	1/3	0.84	20/1	24.3	1.14	572.8
S9	110	4	3/1	0.84	10/1	25.4	1.09	233.5
S10	170	1	1/3	1.26	10/1	14.1	1.15	637.9
S11	110	1	1/3	1.26	20/1	16.5	1.07	748.0
S12	110	1	3/1	1.26	10/1	7.8	0.91	730.7
S13	170	1	1/3	0.84	20/1	12.7	1.08	635.4
S14	170	1	3/1	0.84	10/1	19.6	1.01	588.0
S15	110	1	3/1	0.84	20/1	8.4	0.85	613.4
S16	110	1	1/3	0.84	10/1	13.7	1.15	672.9
S17-I	140	2.5	5/3	1.05	15/1	24.4	0.94	509.8
S17-II	140	2.5	5/3	1.05	15/1	20.8	0.90	473.7
S17-III	140	2.5	5/3	1.05	15/1	25.9	1.27	502.7
S17-IV	140	2.5	5/3	1.05	15/1	26.4	1.07	631.9
S17-V	140	2.5	5/3	1.05	15/1	23.7	0.90	474.7

Solids and water were loaded into the reactor at room temperature; the reactor was sealed and then the sampling cylinder was pressurized with nitrogen to reach the selected pressure ranging from 0.843 to 1.26 MPa. After reaction, the reactor and its contents were cooled to 35 °C; N_2 was released and the reactor disassembled; the mixture was filtered with a 0.45 μm mesh filter and the filter cake was dried in an oven at 105 °C to constant weight, ground and sieved through a 60 μm mesh. The filtrate was analyzed for dissolved calcium by atomic absorption spectroscopy in a Perkin Elmer 1100B atomic absorption spectrometer.

Fig. 1 presents the particle size distribution of the commercial $Ca(OH)_2$, fly-ash and S3 dried hydrated sorbent measured by laser diffraction (Mastersizer X, Malvern Instruments), leading to a mean diameter of 11.78 μm for the sorbent compared to the values of 4.76 m for $Ca(OH)_2$ and 23.44 μm for fly-ash.

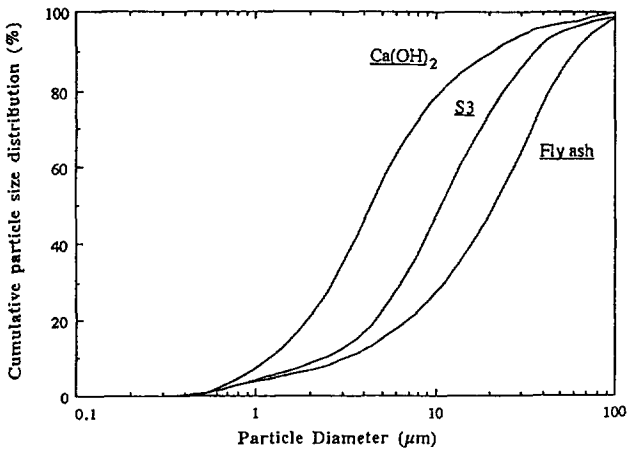

Fig. 1. Cumulative particle size distribution of $Ca(OH)_2$, fly-ash and S3 hydrated sorbent.

Dried solids were tested for BET nitrogen surface area and pore size distribution, using a Micromeritics ASAP-2000 apparatus. The specific surface area (S) was determined following the BET standard method, and pore size distribution was calculated applying the BJH method [40]. The pore volume was determined by the mercury intrusion technique in a Micromeritics Poresizer 9310.

SEM photographs of the hydration products were taken in a Leitz AMR 1000A system with an accelerating voltage of 25.0 kV, in order to observe the macrostructural change due to hydration and sulfation reaction. EDX analysis (Siemens D501) has been used together with SEM in order to study the chemical composition and relative abundance of small areas within a field of particles.

Reactions between sorbents and SO_2 were performed in a glass-made jacketed fixed bed reactor where the sorbent was dispersed into inert silica sand, under isothermal conditions [35,39]. The entire bed was supported on a 3.6 cm diameter fritted glass plate contained in the glass cylinder. A gas stream of 100% SO_2 was passed through the humidification system where the gas was saturated with water vapor in two absorbers of 250 ml each. Both flasks contained small glass spheres in order to improve the contact between gas and liquid phase and were submerged into a water-bath at constant temperature.

After saturation with water, the humidified SO_2 flowed to the reactor through a system of preheated pipes. The reactor

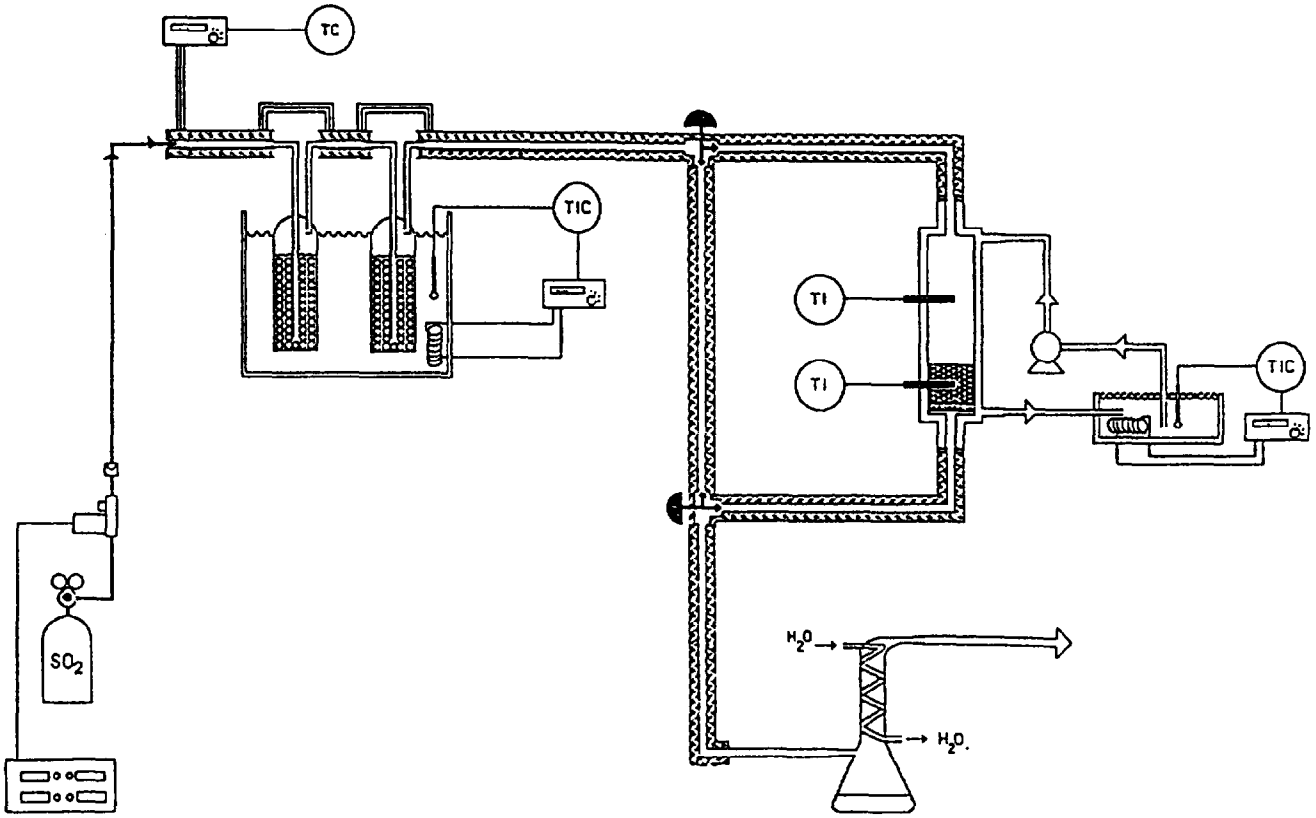

Fig. 2. Experimental set-up for the sulfation test.

was maintained at the reaction temperature by means of hot water passing through the jacket. A schematic diagram of the experimental set-up is shown in Fig. 2. The wet bulb temperature was measured just downstream of the reactor using a wetted wick thermometer. The difference between dry and wet bulb temperatures, that is the "approach to saturation", was used together with the pressure measurement (U tube manometer) to establish the relative humidity under test conditions.

After the reaction time was reached, the experiment was concluded and the entire bed was brought out from the reactor. The solids were sieved to separate the spent sorbent from the inert silica sand ($d_p > 150$ μm) using a Retsch Vibro type sieving unit. The sorbent without inert sand was analyzed by thermogravimetric analysis, in a Perkin-Elmer TGA-7 unit, provided with a high temperature furnace (50–1500°C), a PE 7500 microprocessor and a TAC-7 thermal analysis controller.

TG curves of the reacted calcium hydroxide indicated a mass loss occurring between 850 and 1300°C which was attributed to the sulfate decomposition following the reaction,

$$CaSO_4(s) \xrightarrow{850\text{–}1300°C} CaO(s) + SO_3(g) \quad (1)$$

This analysis allowed the calculation of the amount of SO_2 that had reacted in the bed as SO_4^{-2}. The thermogravimetric analysis of the solid reagent and sulfation products, as well as the complete characterization of the mass loss, have been described elsewhere [41].

3. Results of the hydration runs

A 2^5 fractional factorial design was employed in order to study the influence of hydration variables on the responses, i.e. specific surface area (S), mercury intrusion pore volume (V_p) and dissolved calcium in the filtrate [Ca]. Table 2 shows the experimental design and obtained results. Five experiments (S17-I to S17-V) at the center point of the experimental design were performed in order to determine the experimental error.

In relation to the results of BET specific surface area, two main observations can be mentioned: (i) the obtained values range from 2.5 to 64.3 $m^2\ g^{-1}$; and (ii) the highest value is 64.3 $m^2\ g^{-1}$ corresponding to the experiment S4 performed at the maximum levels of the hydration variables: temperature 170 °C, 4 h reaction time, fly-ash : $Ca(OH)_2$ weight ratio 3 : 1, 1.26 MPa pressure and the minimum level of water : solid ratio = 10 : 1.

Significant variables for the dissolved calcium concentration in the filtrate [Ca] are the fly-ash/$Ca(OH)_2$ weight ratio (FA/CH) and the hydration time (t). This fact has been attributed to the progressive formation of calcium silico-aluminates, as it has been previously mentioned in the literature. Peterson and Rochelle [15,26] correlated the dissolved calcium concentration in the slurry with the solid reactivity, finding an optimum value of this variable (10–100 ppm); these authors reported also that high surface area solids are less reactive when they are formed in slurries containing low concentrations of dissolved calcium.

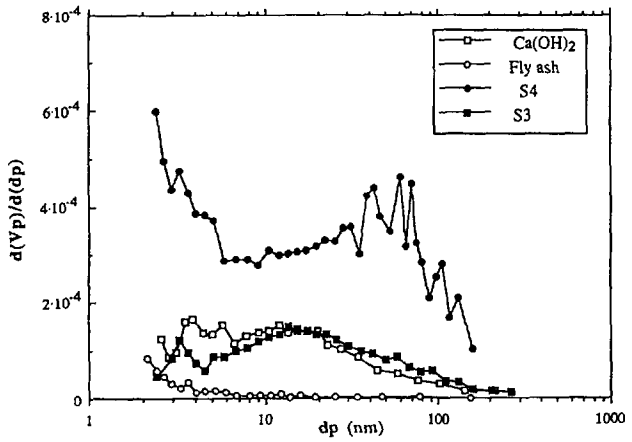

Fig. 3. BJH adsorption pore size distribution of commercial $Ca(OH)_2$, fly-ash and sorbents S3 and S4.

Table 3
Pore volumes and average diameters, obtained by nitrogen adsorption, of initial reagents, S3 and S4 hydrated sorbents and S3p sulfation product

Solid	V_p ($cm^3\ g^{-1}$)	Average pore diameter (nm)	BJH adsorption average pore diameter (nm)
$Ca(OH)_2$	0.07918	20.18	23.78
Fly-ash	0.00455	6.79	13.08
S4	0.33883	21.37	–
S3	0.08869	19.58	31.76
S3p	0.03634	14.17	30.65

Fig. 4. SEM micrograph of the S3 hydrated sorbent prior to the sulfation reaction (the white line indicates 0.1 mm).

The observed difference between the maximum and minimum values of the total pore volume, obtained by the mercury intrusion technique, lies within the range of the experimental error. Therefore, an average value of the parameter, V_{total}: $1.077 \pm 0.066\ cm^3\ g^{-1}$, was taken as representative. Thus, it was concluded that the selected hydration variables have no influence on the hydrated solids pore volume, attributing the increase of the specific surface area in the hydrated solids to the generation of very fine pores that are not detectable by mercury intrusion porosimetry.

Working with hydrated lime, in a previous work [35] the region of pore sizes between 9 and 200 nm has been identified as the effective zone in the sulfation reaction, so special attention has been paid to the latter region. The "BJH" procedure, which permits a better characterization of mesoporosity, was applied to obtain the mesopore size distribution from nitrogen adsorption data using the adsorption branch of the hysteresis loop. Pore size distribution represented by the derivative $d(V_p)/d(dp)$ as a function of dp is shown in Fig. 3 for $Ca(OH)_2$, fly-ash, S3 hydrate (BET specific surface area similar to $Ca(OH)_2$) and S4 hydrate (maximum value of BET specific surface area). Table 3 summarizes the pore volume data, considering the volume of pores with a diameter smaller than 100 nm, and the results of mean pore diameter obtained from nitrogen adsorption data.

Fig. 4 shows the SEM micrograph of the S3 hydrated sorbent prior to the sulfation reaction. The spherical particles of fly-ash seem to be surrounded by a rough surface due to the reaction of fly-ash species with $Ca(OH)_2$, they are frequently embedded in the $Ca(OH)_2$ matrix. Sphere-like ash particles contain Si, Al, Ca, Fe, Ti and K. Particles of less sphericity, compact blocks and agglomerates containing ash spheres are observed and exhibit higher relative abundance of calcium than other elements. The SEM micrographs of the other hydrated sorbents (S1–S17) show similar characteristics with different fractions of isolated ash particles and agglomerates.

Referring to the hydrated sorbents, several investigations remarked the effect of hydration conditions on sorbent morphology and composition [11,17,20–22,26,42]. Jozewicz and Chang [38] suggested that two factors were necessary in a sorbent to readily react with SO_2 under the conditions encountered in a dry injection FGD process: (i) sorbent surface area, and (ii) amorphous surface structure. Both factors could be optimized by a careful selection of the time/temperature conditions in the pressurized hydration for a selected fly-ash-to-$Ca(OH)_2$ weight ratio. More recently, Sanders et al. [23] pointed out the importance of bound water in the silicates, the morphology and the crystallinity, considering them as relevant factors affecting the sulfation rate.

4. SO_2 reaction test results and discussion

The sulfation tests were performed using a pure gas, (SO_2 saturated with water), under reaction conditions given in

Table 4
Experimental conditions of the SO_2 reaction test

SO_2 (saturated with water)	100%
Reaction temperature	57 °C
Relative humidity	90%
Solid reagent	S1–S17 sorbents
Sorbent weight	2 g
Inert	Silica
Inert size	> 150 μm
Sorbent/inert ratio	1/25
Gas flow rate	30 N $cm^3\ min^{-1}$
Reaction time	1, 4 and 8 h

Table 4. Reactions using the mixed solids obtained previously in the hydration runs were carried out at reaction times, 1, 4 and 8 h. in order to analyze the influence of this variable on the sulfation yield.

Taking into account previous works [13,14,27,28] and in order to obtain comparable results, the SO_2 retention capacity of the hydrated solids towards SO_2 was expressed in two forms; (i) R_1 or SO_2 capture, defined as the total number of millimoles of SO_2 removed per g sorbent (mmol SO_2 per g sorbent) (Eq. (2)), and (ii) R_2 or conversion, defined as the total number of moles of SO_2 removed divided by the initial number of moles of Ca (mol SO_2 per mol Ca) (Eq. (3)). SO_2 capture, R_1, may be helpful when evaluating the commercial application of a sorbent injected into the duct leading to an existing particulate control device.

$$R_1 = \frac{\text{mmol } SO_2}{\text{g sorbent}} = \frac{\text{mmol } SO_2}{\text{g product}} \times \frac{\text{g product}}{\text{g sorbent}} \quad (2)$$

$$R_2 = \frac{\text{mol } SO_2}{\text{mol Ca}} = \frac{\text{mol } SO_2}{\text{g sorbent}} \times \frac{\text{g product}}{\text{g sorbent}} \times \frac{\text{g sorbent}}{\text{mol Ca}} \quad (3)$$

The first term of Eqs. (2) and (3), that is, the amount of SO_2 referring to the final product (mol SO_2 per g product) was calculated from the thermogravimetric analysis at high temperature, taking into account the weight loss in the temperature range 850–1300 °C, which can be attributed to sulfate decomposition (SO_3). The stability of the reagents at these temperatures was checked previously obtaining a final mass loss negligible in all sorbents ($< 1.1\%$).

After the sulfation experiment was concluded, the final product was sieved from the silica sand and weighed to find the weight increase and the product-to-sorbent ratio (g product per g sorbent). The term, mol Ca per g sorbent, was calculated from the difference between the theoretical amount of Ca (mol) in the pressurized hydration reactor and the solubilized Ca in the filtrate as a consequence of the hydration process.

Table 5 summarizes the weight losses of the sulfation products S1p to S17p in the range of 850–1300 °C obtained by TGA, and the different terms of Eqs. (2) and (3).

Sorbent conversion, R_2, obtained after one hour of reaction did not reveal a significant influence on the fly-ash/$Ca(OH)_2$ weight ratio, obtaining an average value of 0.49 ± 0.08 mol SO_2 per mol Ca (excluding S5p and S7p which presented extremely low conversion values). Taking into account the conclusions reported previously concerning the desulfurization behavior of $Ca(OH)_2$ [33,36], which under similar experimental conditions led to a maximum conversion of 0.62 mol SO_2 per mol Ca, it was thought necessary to study the possible evolution of sorbent conversion at longer sulfation times (4 and 8 h).

Fig. 5 represents the evolution of R_2 for S1 to S17 sorbents at 1, 4 and 8 h sulfation time, together with the conversion of calcium hydroxide (0.62 mol SO_2 per mol Ca) and of fly-ash (0.06 mol SO_2 per mol Ca). The average conversion value for the sorbents was 0.56 ± 0.07 mol SO_2 per mol Ca, very similar to the $Ca(OH)_2$ conversion.

Fig. 6 represents the evolution of the solid conversion with the BET specific surface area. Whereas sorbents S5 and S7 presented the lowest values of specific surface area (2.5 and 3.1 $m^2 g^{-1}$, respectively) and the lowest values of conversion (0.17 and 0.14 mol SO_2 per mol Ca, respectively), no effect of the BET specific surface area on sorbent utilization was found; thus, it was concluded that sorbents with potentially better structures did not lead to significantly enhanced conversions compared with the SO_2 capture per mol of calcium.

Fig. 7 shows the changes in pore volume distribution obtained from nitrogen adsorption for samples S3 and S3p.

Table 5
Summary of reactivities R_1 and R_2 for sulfation products (S1p–S17p)

Product	Weight loss (850–1300°C) (%)	mmol SO_2 / g product	g product / g sorbent	g sorbent / mol Ca	R_1 mmol SO_2 / g sorbent	R_2 mmol SO_2 / mol Ca (%)
S1p	10.85	1.356	1.074	334.5	1.456	48.71
S2p	9.27	1.159	1.046	309.1	1.213	37.50
S3p	12.83	1.624	1.086	322.5	1.764	56.90
S4p	13.25	1.656	1.091	308.7	1.807	55.77
S5p	11.76	1.469	1.024	110.3	1.505	16.60
S6p	27.07	3.375	1.114	108.1	3.760	40.71
S7p	10.01	1.251	1.026	108.1	1.283	13.86
S8p	31.31	3.916	1.167	109.7	4.570	50.14
S9p	11.23	1.443	1.095	110.8	1.580	49.70
S10p	33.26	4.162	1.247	108.2	5.190	56.18
S11p	27.66	3.459	1.203	831.6	4.160	46.10
S12p	12.11	1.514	1.087	327.0	1.645	53.80
S13p	27.97	3.505	1.255	110.1	4.400	48.40
S14p	12.97	1.621	1.129	323.2	1.830	59.16
S15p	11.11	1.385	1.090	340.8	1.510	51.50
S16p	27.14	3.395	1.143	108.3	3.880	42.00
S17p	19.04	2.379	1.178	218.1	2.808	61.17

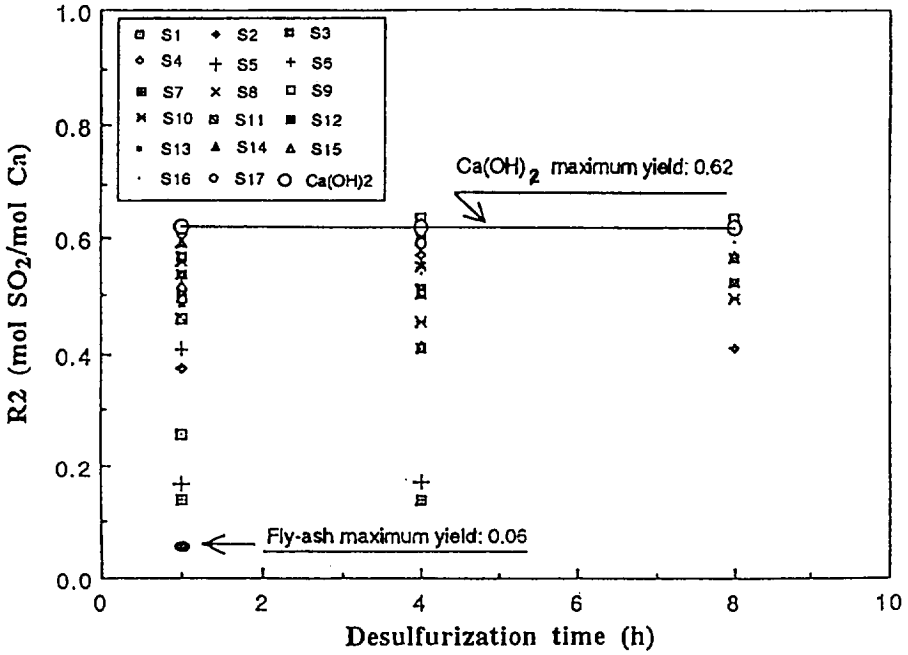

Fig. 5. Calcium conversion of samples S1 to S17 for sulfation times of 1, 4 and 8 h.

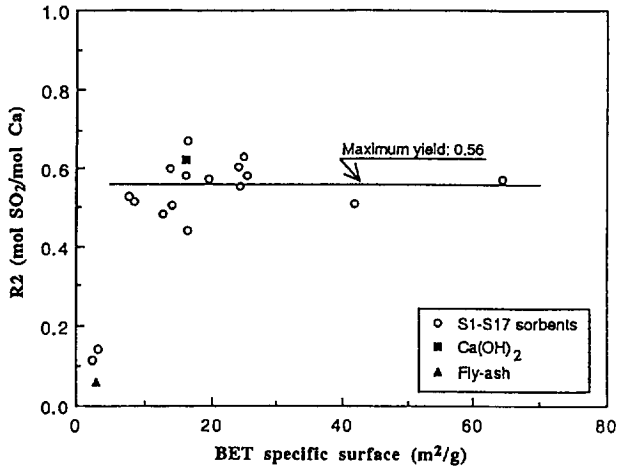

Fig. 6. Calcium conversion as a function of the BET specific surface area.

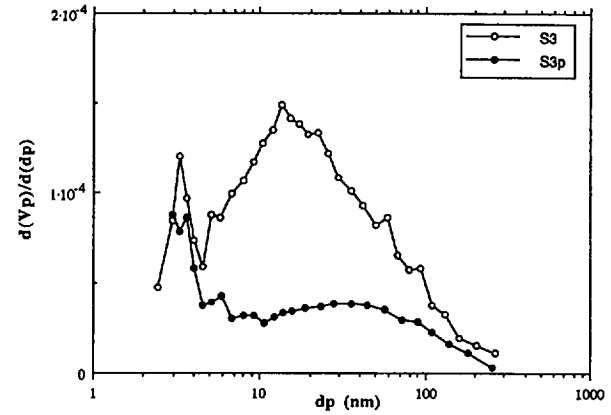

Fig. 7. BJH adsorption pore size distribution of S3 hydrated sorbent prior to sulfation and after sulfation reaction (S3p).

The sulfation reaction causes a dramatic decrease in the mesopore volume (see Table 3), confirming that the region of pore sizes between 2 and 100 nm is the changing zone in the sulfation reaction as it has been reported previously by Ortiz et al. [35].

A reasonable correlation between the SO_2 capture R_1 and the hydration fly-ash/$Ca(OH)_2$ (FA/CH) weight ratio was obtained (Eq. (4)) indicating that as the FA/CH ratio increased, there was a corresponding decrease in the SO_2 capture R_1 per g of solid sorbent.

$$R_1\left(\frac{\text{mmol } SO_2}{\text{g sorbent}}\right)=5.48-1.26\left(\frac{FA}{CH}\right) \quad (4)$$

$r^2=0.99$

The experimental behavior of R_1 and R_2 pointed out a strong dependence of the sulfation yield on the amount of calcium in the sorbents, rather than on the type and structure of the calcium species in the hydrated solid.

SEM micrographs taken of the sulfated solids corroborated this finding, showing that no significant changes in the external surface of these particles took place with respect to the hydrated sorbent prior to the reaction, that is, the Ca matrix was embedded by ash spheres. Fig. 8 represents the SEM micrograph of the sulfated product S3p, where two different areas, 1 and 2, were selected for the EDX spectra, showing a heterogeneous distribution of calcium and sulfur in the particle.

5. Conclusions

In this work structural properties have been studied, i.e., the specific surface and pore volume, of the mixed solids

Fig. 8. SEM micrograph of the fly-ash sample hydrated with $Ca(OH)_2$ after sulfation reaction (S3p) (the white line indicates 10 μm).

obtained after pressurized hydration of $Ca(OH)_2$ and fly-ashes have been determined. Hydration experiments planned according to a 2^5 experimental design, allow to study the influence of the variables: temperature (110–170 °C), time (1–4 h), fly-ash : $Ca(OH)_2$ weight ratio (1 : 3–3 : 1), pressure (0.843–1.26 MPa) and water : solid ratio (10 : 1–20 : 1), considering as objective functions the structural properties, specific surface area and pore volume, and the dissolved calcium concentration in the slurries.

The determination of the BET specific surface area led to the conclusion that a considerable generation of surface takes place due to the generation of very fine pores, in the pressurized hydration of fly-ash ($S=2.9$ m^2 g^{-1}) and calcium hydroxide ($S=16.2$ m^2 g^{-1}). The obtained values ranged from 2.5 to 64.3 $m^2 g^{-1}$, and this increase was directly related to the individual influences of the weight ratio of fly-ash to $Ca(OH)_2$ and the hydration time.

The dissolved calcium content in the slurry filtrate after hydration varied inversely with hydration time and fly-ash/$Ca(OH)_2$ weight ratio; this finding is explained by the formation of calcium silico-aluminate species.

The reactivity of the obtained sorbents was tested with pure SO_2 in a packed bed reactor at 57 °C and 90% relative humidity. The conversion values obtained after 1 h of reaction time showed an average conversion of 0.49 ± 0.08 mol SO_2 per mol Ca, and a capture of SO_2 per g of sorbent dependent on the fly-ash/$Ca(OH)_2$ weight ratio. Long time sulfation tests (4 and 8 h) led to a calcium utilization of 0.56 ± 0.07 mol SO_2 per mol Ca, very similar to the maximum conversion previously determined with commercial $Ca(OH)_2$ (0.62 mol SO_2 per mol Ca). These results led to the conclusion that the calcium content in the sorbent composition is the relevant parameter in the solid utilization.

The relationship between BET specific surface area and sorbent utilization was evaluated, in order to clarify the discrepancies reported in the literature referring to the influence of this variable. The obtained results verified that the created additional surface area and the formation of new calcium species did not lead to an additional sulfation capacity.

Acknowledgements

This work has been financially supported by the Spanish CICYT under Project No. AMB 94-0991-CP.

References

[1] L. Muzio, G. Offen, JAPCA 37 (5) (1987) 642.
[2] G. Offen, M. McElroy, L. Muzio, JAPCA 37 (1987) 968.
[3] R. Dennis, N. Ford, M. Cooke, IChemE Symp. Ser. 131 (1993) 119.
[4] D. Ablin, J. Hammond, D. Watts, R. Ostop, 100 MW demonstration of dry sodium injection flue gas desulfurization, in: B. Emmel, J. Jones, R. Moser (Eds.), Proc. 10th Symp. on Flue Gas Desulfurization, vol. 7, Atlanta, 1987.
[5] M. Garding, G. Svedberg, JAPCA 38 (1988) 1275.
[6] H. Karlsson, J. Klingspor, M. Linné, I. Bjerle, JAPCA 33 (1) (1983) 23.
[7] R. Ruiz-Alsop, G. Rochelle, effect of deliquescent salt additives on the reaction of SO_2 with dry $Ca(OH)_2$, ACS Symp. Ser. 319 (1986) 208.
[8] C. Jorgensen, J. Chang, T. Brna, Environ. Prog. 6 (1987) 26.
[9] P. Farber, C. Livengood, Characterization of an industrial spray dryer at Argonne National Laboratory, in: F. Ayer, J. Jones, T. Morasky (Eds.), Proc. 8th Symp. on Flue Gas Desulfurization, vol. 2, New Orleans, 1984, p. 10.
[10] W. Jozewicz, J. Chang, T. Brna, C. Sedman, Environ. Sci. Technol. 21 (7) (1987) 664.
[11] J. Peterson, G. Rochelle, Lime/flash materials for FGD: effects of aluminum and recycle materials, in: C. Sedman, P. Radcliffe (Eds.), Proc. 1990 SO_2 Control Symp., vol. 4, New Orleans, 1991, p. P-3.
[12] K. Svoboda, J. Nannes, W. Lin, C. van den Bleek, IChemE Symp. Ser. 131 (1993) 253.
[13] W. Jozewicz, C. Jorgensen, J. Chang, C. Sedman, T. Brna, JAPCA 38 (6) (1988) 796.
[14] W. Jozewicz, J. Chang, C. Sedman, T. Brna, JAPCA 38 (1988) 1027.
[15] L.B. Clarke, Applications for Coal-Use Residues, IEA Coal Research, London, 1992.
[16] R.W. Row, Waste Management 14 (3/4) (1994) 299.
[17] W. Jozewicz, G. Rochelle, Environ. Prog. 5 (4) (1986) 219.
[18] P. Chu, G. Rochelle, JAPCA 39 (2) (1989) 175.
[19] B. Hall, C. Singer, W. Jozewicz, C. Sedman, M. Maxwell, J. Air Waste Management 42 (1992) 103.
[20] C. Ho, S. Shih, Ind. Eng. Chem. Res. 31 (4) (1992) 1130.
[21] A. Al-Shawabkeh, H. Matsuda, M. Hasatani, J. Chem. Eng. Jpn. 28 (1) (1995) 302.
[22] H. Tsuchiai, T. Ishizuka, T. Ueno, H. Hattori, H. Kita, Ind. Eng. Chem. Res. 34 (1995) 1404.
[23] J. Sanders, T. Keener, J. Wang, Ind. Eng. Chem. Res. 34 (1995) 302.
[24] G. Reed, W. Davis, R. Pudelek, Environ. Sci. Technol. 18 (1984) 548.
[25] J. Izquierdo, F. Cunill, J. Martinez, J. Tejero, A. Garcia, Separat. Sci. Technol. 27 (1992) 61.
[26] J. Peterson, G. Rochelle, Environ. Sci. Technol. 22 (11) (1988) 1299.
[27] P. Diffenbach, M. Hilterman, E. Frommell, H. Booher, S. Hedges, Thermochim. Acta 189 (1991) 1.
[28] J. Martinez, J. Izquierdo, F. Cunill, J. Tejero, J. Querol, Ind. Eng. Chem. Res. 30 (9) (1991) 2143.
[29] G. Rochelle, W. White, W. Jozewicz, J. Chang, Reaction of hydrated lime with SO_2 in humidified flue gas, in: C. Sedman, P. Radcliffe (Eds.), Proc. 1990 SO_2 Control Symp., vol. 4, New Orleans, 1991, p. 7A-119.
[30] J. Klingspor, H. Karlsson, I. Bjerle, Chem. Eng. Commun. 22 (1983) 81.
[31] J. Klingspor, A. Stromberg, H. Karlsson, I. Bjerle, Chem. Eng. Prog. 18 (1984) 239.

[32] K. Murphy, E. Samuel, H. Pennline, Current status of in-duct scrubbing technology, in: B. Emmel, J. Jones, R. Moser (Eds.), Proc. 10th Symp. on Flue Gas Desulfurization, vol. 2, Atlanta, 1987, p. 9.
[33] F. Cortabitarte, I. Ortiz, A. Irabien, Thermochim. Acta 207 (1992) 255.
[34] A. Irabien, F. Cortabitarte, I. Ortiz, Chem. Eng. Sci. 47 (1992) 1533.
[35] I. Ortiz, F. Cortabitarte, A. Garea, A. Irabien, Powder Technol. 75 (1993) 167.
[36] I. Ortiz, A. Garea, I. Fernandez, A. Oliván, J. Viguri, A. Irabien, On the kinetic modeling of the FGD reaction at low temperatures, in: R. Owens, B. Gullet (Eds.), Proc. 1993 SO_2 Control Symp., vol. I, Boston, 1993.
[37] C. Singer, W. Jozewizc, C.B. Sedman, Suitability of available fly ashes in advacate sorbents, in: Proc. 1991 SO_2 Control Symp., Washington DC, 1991.
[38] W. Jozewicz, J.C.S. Chang, Evaluation of FGD injection sorbents and additives, vol. I. Development of high reactivity sorbents, EPA-600/7-89-006a, 1989.
[39] A. Irabien, I. Ortiz, F. Cortabitarte, A. Garea, J. Viguri, IChemE Symp. Ser. 131 (1993) 229.
[40] E.P. Barret, L.S. Joyner, P.P. Halende, J. Am. Chem. Sci. 73 (1951) 373.
[41] A. Garea, I. Ortiz, J. Viguri, M.J. Renedo, J. Fernandez, A. Irabien, Thermochim. Acta , 286 (1996) 173.
[42] J.U. Otaigbe, N.O. Egiebor, Thermochim. Acta 195 (1992) 183.